PAPR Reduction and Channel Estimation for FBMC/OQAM Systems

A project report
submitted by

Vivek Kumar Gupta
(EE11B079)

under the guidance of

Prof. Ravinder David Koilpillai

in partial fulfilment of the requirements
for the award of the degree of

MASTER OF TECHNOLOGY

DEPARTMENT OF ELECTRICAL ENGINEERING
INDIAN INSTITUTE OF TECHNOLOGY MADRAS
May 2016

THESIS CERTIFICATE

This is to certify that the thesis titled **PAPR reduction and Channel Estimation for FBMC/OQAM Systems**, submitted by **Vivek Kumar Gupta**, to the Indian Institute of Technology, Madras, for the award of the degree of **Master of Technology,** is a bonafide record of the research work done by him under my supervision. The contents of this thesis, in full or in parts, have not been submitted to any other Institute or University for the award of any degree or diploma.

Prof. R. David Koilpillai
Research Guide
Professor
Dept. of Electrical Engineering
IIT-Madras, 600 036
Place: Chennai

Date: 8th June 2016

ACKNOWLEDGEMENTS

I express my sincere gratitude to Prof. R. David Koilpillai, who has given me more knowledge and skills in the DSP and communication field. In addition, his guidance helped me throughout this research and the writing of this thesis.

I would like to take this opportunity to express my deepest appreciation to my family especially my parents, for the endless care they have provided me, advices, support and patience.

My deep gratitude goes to all my friends, especially at Indian Institute of Technology, Madras.

I would also like to thank to all those who helped me during the period of my study and gave me motivation and encouragement.

ABSTRACT

KEYWORDS: FBMC-OQAM, OFDM, Peak-to-Average Power Ratio (PAPR), Selected Mapping (SLM), Dispersive SLM, Least Squares (LS), Minimum Mean Square Error (MMSE), LMS, Mean Squared Error (MSE)

Filter Bank Multi-Carrier Offset Quadrature Amplitude Modulation (FBMC-OQAM) based systems are being used widely for multi-carrier communications. Compare to Orthogonal Frequency Division Multiplexing (OFDM), FBMC-OQAM has got several advantages like increased data rate, low out of band radiation and good spectral efficiency etc. As FBMC-OQAM is a multi-carrier technique, it suffers from the high Peak-to-Average Power Ratio (PAPR). High PAPR means more power need at transmission side. There are various methods to reduce the PAPR in multi-carrier modulation (like OFDM) techniques like clipping, selected mapping (SLM), partial transmit sequence (PTS) etc. The PAPR reduction methods of OFDM turn out to be ineffective in case of FBMC-OQAM. Because, the FBMC-OQAM signals has an overlapping structure.

This thesis deals with the problem of high Peak-to-Average Power Ratio (PAPR) in FBMC-OQAM systems. A modified Selected Mapping (SLM), named Dispersive Selected Mapping (DSLM) is used to reduce PAPR of FBMC-OQAM signals. DSLM method is an extended and generalized version of Overlapped Selected Mapping (OSLM). Dispersive SLM technique accords with the time dispersive characteristics of the FBMC-OQAM signals.

In this contribution, we will deal with the problem of channel estimation and equalization techniques in FBMC-OQAM systems. Channel estimation is a very important step to deal in multi-carrier communications. We present the problem of estimating fading channels in FBMC-OQAM systems based on pilot symbols. The least squares (LS) estimator and the minimum mean square error

(MMSE) estimator, with possible adaptive implementation using least mean square (LMS), is used to tackle the problem of channel estimation.

To solve the problem of channel equalization, we design an adaptive channel equalization algorithm for FBMC-OQAM systems based on least mean square (LMS) method. This presented technique will be optimized based on cost functions, which is the mean squared error (MSE).

TABLE OF CONTENTS

LIST OF TABLES

LIST OF FIGURES

CHAPTER 1

INTRODUCTION

Multi-carrier communication is an efficient transmission technique, where the available channel bandwidth is subdivided into several parallel sub-channels, each with its own associated carrier. In addition, the division of the whole bandwidth into many sub-channels gives the advantage of scalability and flexibility when designing the communication link. FBMC is a new waveform technique having few advantages over OFDM, a potential contender for 5G. The only fundamental change is the replacement of the OFDM with a multicarrier system based on filter banks at the transmitter (Tx) and Receiver (Rx).

OFDM suffers the bandwidth (BW) efficiency because OFDM is a cyclic prefix (CP) based multi-carrier block modulation technique. But, FBMC does not use cyclic prefix (CP) extension resulting in better use of the allocated spectrum and conserving bandwidth (BW). OFDM's frequency spectrum contains large side-lobes compared to FBMC system. OFDM system is highly sensitive to the carrier frequency offset. But, FBMC system is less sensitive to the carrier frequency offset and hence it performs significantly with the increase of the user mobility in FBMC system. OFDM system has also high flexibility while adopting multiple input multiple output (MIMO) techniques. FBMC system has low flexibility while adopting MIMO techniques. OFDM signals have degraded spectrum sensing performance due to the spectral leakage. FBMC signals have high spectrum sensing performance due to better allocated spectrum. OFDM system has less complexity than FBMC system in implementation.

A prototype filter (Phydyas Filter) designed with the Nyquist pulse shaping criterion is adopted, which can largely reduce the spectral leakage problem of

OFDM system. To get a maximum data transmission rate, we use offset quadrature amplitude modulation (FBMC-OQAM) with filter banks.

FBMC-OQAM system suffers from an inter-symbol interference, which complicates receiver tasks that can be done easily in OFDM using cyclic prefix (CP). There is a lot more method of channel estimation using pilot/training designs. A very large number of estimation techniques have been developed for multi-carrier communication systems. The Least Square (LS) estimation is trivial, but it remains very sensitive to noise. But, the optimal estimator is the linear minimum mean square error (LMMSE) method. It is very effective to cancel the interferences and noise since it acts like a smoothing step but has a very high computational complexity that makes it difficult to implement. In addition, it requires prior knowledge of the channel covariance matrix to achieve noise mitigation.

CHAPTER 2

Filter Bank Multi-Carrier (FBMC-OQAM) Systems Model

In FBMC, a set of parallel data symbols $s_k[n]$ are transmitted through a bank of modulated filters and it is synthesized by equation given below. The main difference between OFDM and FBMC lies in the choice of the prototype filters $p_T(t)$ and $p_R(t)$. Also, the selection of $p_T(t)$ and $p_R(t)$ varies depending on the adopted FBMC modulation technique. We can describe two types of FBMC systems. The first type is that we introduce are designed to transmit complex-valued (QAM) data symbols. The second type of FBMC systems that will be introduced are designed to transmit real-valued (PAM) data symbols. In FBMC, the receiver uses a prototype filter $p_R(t)$ that is matched to the transmit prototype filter $p_T(t)$, i.e., $p_R(t) = p_T(-t)$, and most of the design methods that have been proposed to consider symmetric prototype filter, i.e., $p_T(t) = p_T(-t) = p_R(t)$.

$$x(t) = \sum_{n} \sum_{k\ e\ K} s_k[n]\, p_T(t - nT) \exp(j2\pi(t - nT) f_k)$$

2.1 FBMC-OQAM Model

The general structure of FBMC/OQAM wireless system is shown in the below figures which consists of several main processing blocks. At the transmitter side, it consists of OQAM pre-processing and synthesis filter bank (SFB). At the

receiver side, it consists of analysis filter bank (AFB), channel estimation and equalization block and OQAM post-processing.

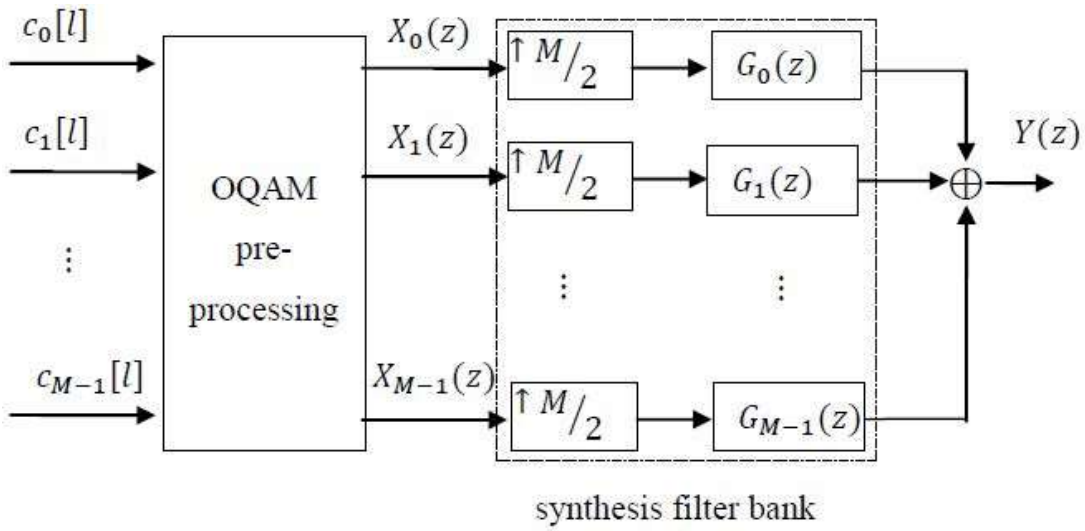

Figure 2.1: Transmitter side: General block diagram of FBMC/OQAM system

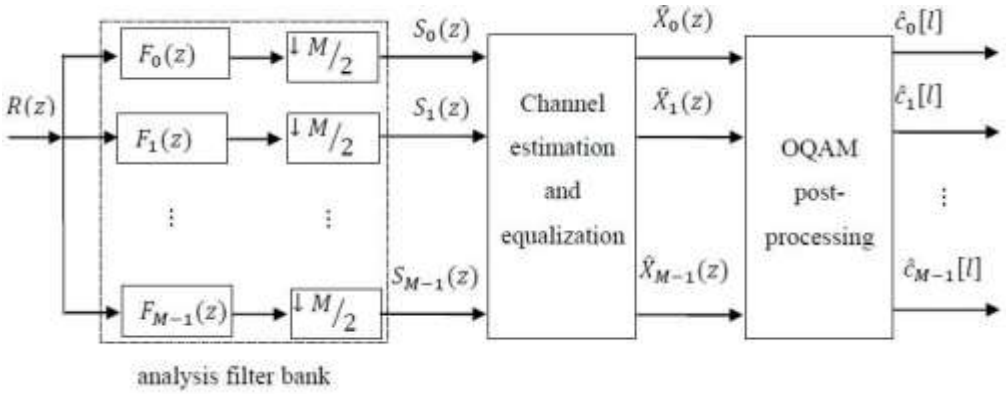

Figure 2.2: Receiver side: General block diagram of FBMC/OQAM system

2.1.1 OQAM pre-processing block

Unlike other multi-carrier communication, OQAM symbols are transmitted rather than QAM symbols. To achieve this modulation, we have used pre/post-processing blocks at the transmitter/receiver sides, respectively. The pre-

processing block, which utilizes the transformation between QAM and OQAM symbols, is shown. As we can see, the first operation is a simple complex-to-real conversion, where the real and imaginary parts of a complex-valued symbol $c_k[l]$, transmitted at a rate of $1/T$ where the signalling period is defined as $T = 1/\Delta f$ with Δf is the subcarrier spacing, are separated to form two new symbols $d_k[n]$ and $d_k[n+1]$. This operation generally can be called as staggering. The complex-to-real conversion is different for even and odd numbered sub-channels and can be written by the following equations:

$$d_k[n] = \{\, Re(c_k[l]), when\ k\ is\ even\ else\ Im(c_k[l])$$

$$d_k[n+1] = \{\, Im(c_k[l]), when\ k\ is\ even\ else\ Re(c_k[l])$$

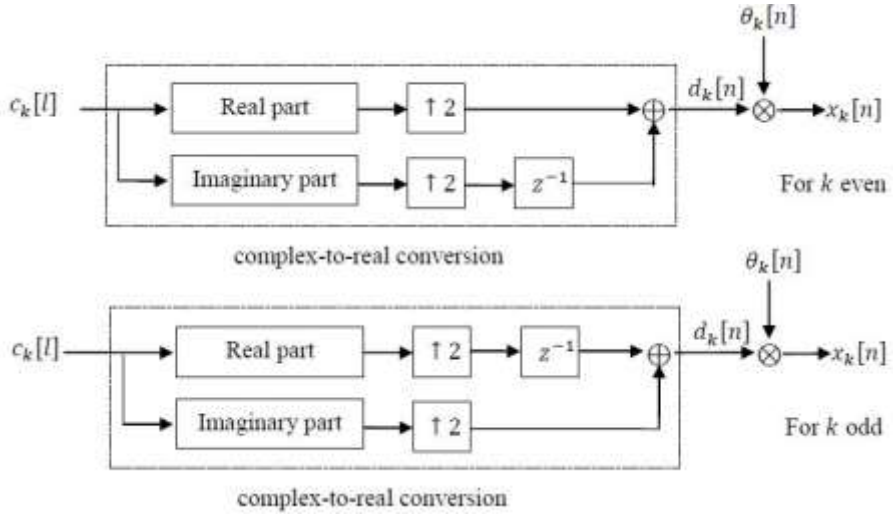

Figure 2.3: OQAM pre-processing

Where, $l = sample\ index\ at\ OQAM\ pre-processing\ input\ and\ post-processing\ output$

$$n = sample\ index\ at\ OQAM\ pre-processing\ output\ and\ post-processing\ input$$

Also, we can see that complex-to-real conversion increases the sample rate by factor 2. The second operation of the OQAM pre-processing block is the multiplication by $\Theta_k[n]$ in order to maintain orthogonal symbols.

$$\Theta_k[n] = j^{k+n}$$

So, the output data of the pre-processing block $x_k(n)$ can be expressed as:

$$x_k[n] = d_k[n]\Theta_k[n]$$

2.1.2 OQAM post-processing block

The block diagram of the OQAM post-processing is shown in following figure. It also consists of two main operations opposite of pre-processing. In first part, we multiply by the complex conjugate of $\Theta_k[n]$ then take the real part of it. In second part, real-to-complex conversion takes place, in which two successive real valued symbols form a complex valued symbol denoted by $c_k'[l]$ and defined as:

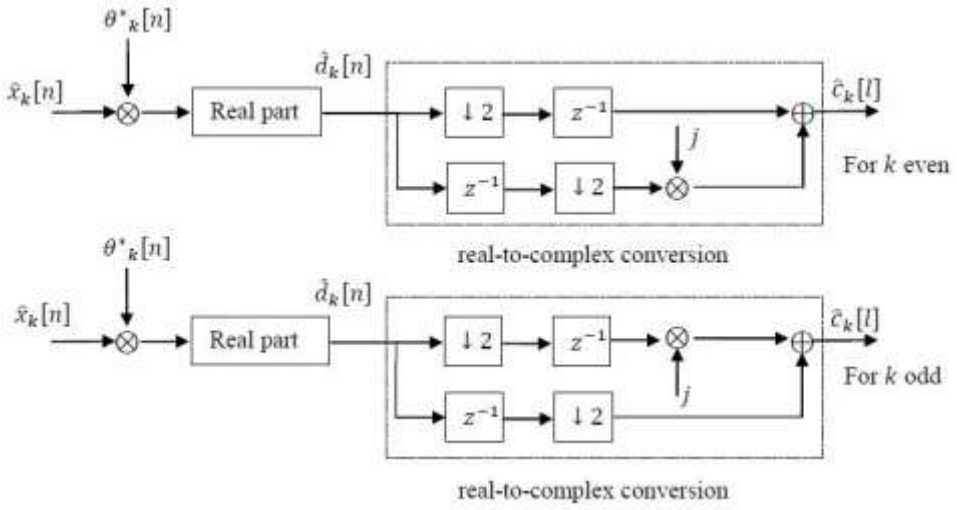

Figure 2.4: OQAM post-processing

$$c_k'[l] = d_k'[n] + jd_k'[n+1], when\ k\ is\ even\ else\ d_k'[n+1] + jd_k'[n]$$

As we can see, In this sense the real-to-complex conversion decreases the sample rate by factor 2.

2.1.3 Synthesis and Analysis Filter Bank Blocks:

At the transmitter, M up-samplers and M synthesis filters will form synthesis filter bank. The data $X_k(z)$ is then up sampled $M/2$ by and filtered with synthesis filters $G_k(z)$. Finally all sub-channels are added together to form $Y(z)$. At the receiver, M down-samplers and M analysis filters will form analysis filter bank such that the signal $R(z)$ is filtered with analysis filters $F_k(z)$, and then down sampled by $M/2$ to form $X'_k(z)$.
In order to achieve high spectral efficiency, complex modulated filter banks are usually used. This means that all sub-channel filters are frequency shifted versions of a single real-valued linear-phase finite impulse response (FIR) low-pass prototype filter by using exponential modulation. Thus, the synthesis filter can be expressed as:

$$g_k[m] = p[m]\exp(\frac{j2\pi k}{M}\left(m - \frac{L_p - 1}{2}\right))$$

Where $m = 0,1,\dots,L_p - 1$, M is the number of sub-channels (typically a power of two), and L_p is the prototype filter length which is chosen to be $L_p = KM - 1$, where K is overlapping factor.

We can design analysis filter $f_k[m]$ easily from synthesis filter itself. The k^{th} analysis filter $f_k[m]$ is a time reversed and complex-conjugated version of the corresponding synthesis filter.

$$f_k[m] = g_k{}^*\,[L_p - 1 - m]$$

After some algebra, we can write above equation as:

$$f_k[m] = p[L_p - 1 - m]\exp(\frac{j2\pi k}{M}\left(m - \frac{L_p - 1}{2}\right))$$

Due to the nature of the modulation function, the $0th$ sub-channel filter is purely real and the $M/2th$ is purely imaginary. However, all the sub-channel filters have linear phase.

2.3 Design of Prototype Filter:

We will design prototype filters which will satisfy nearly perfect reconstruction (NPR) characteristics beacause perfect reconstruction (PR) property is only achieved under the condition of ideal transmission channel. There are different approach to design NPR prototype filter like windowing based techniques or frequency sampling technique. We have focused on fraquency sampling technique to achieve this target.

The impulse response coefficients of the filter are obtained according to the desired frequency response, which is sampled on a KM uniformly spaced frequency points $w_k = \frac{2\pi k}{KM}$. So, we can write the FIR low-pass prototype filter $p[m]$ as:

$$p[m] = \frac{1}{KM}\left(P'[0] + 2\sum_{k=1}^{U}(-1)^k P'[k] cos\left(\frac{2\pi k}{KM}(m+1)\right)\right)$$

Where $m = 0,1,\dots,L_p - 1$, and

$$P'[0] = 1$$

$$P'[k]^2 + P'[K-k]^2 = 1, \quad for\ k = 1,2,\dots,\frac{K}{2}$$

$$\mathrm{P'[k]} = 0, \quad for\ k = K, K+1, \dots, U = \frac{KM-2}{2}$$

The frequency response and the impulse response for the prototype filter used in FBMC/OQAM wireless system with different values of overlapping factor are shown in following figures.

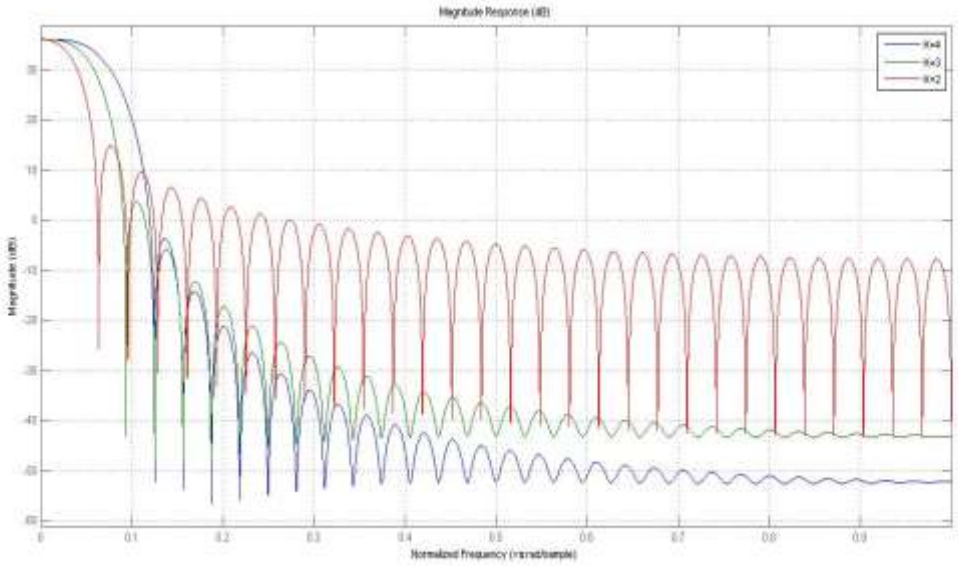

Figure 2.5: Frequency response of prototype filter of different overlapping factor (FBMC/OQAM)

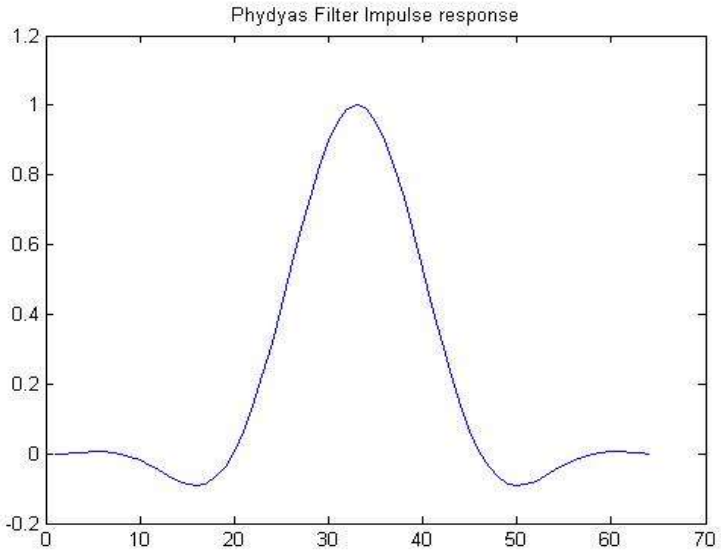

Figure 2.6: Impulse response of prototype filter of FBMC/OQAM for K=4

The following figure consist the frequency response of Phydyas or FBMC prototype filter and OFDM prototype filter. And we can verify that frequency response of OFDM has higher side-lobes than frequency response of FBMC.

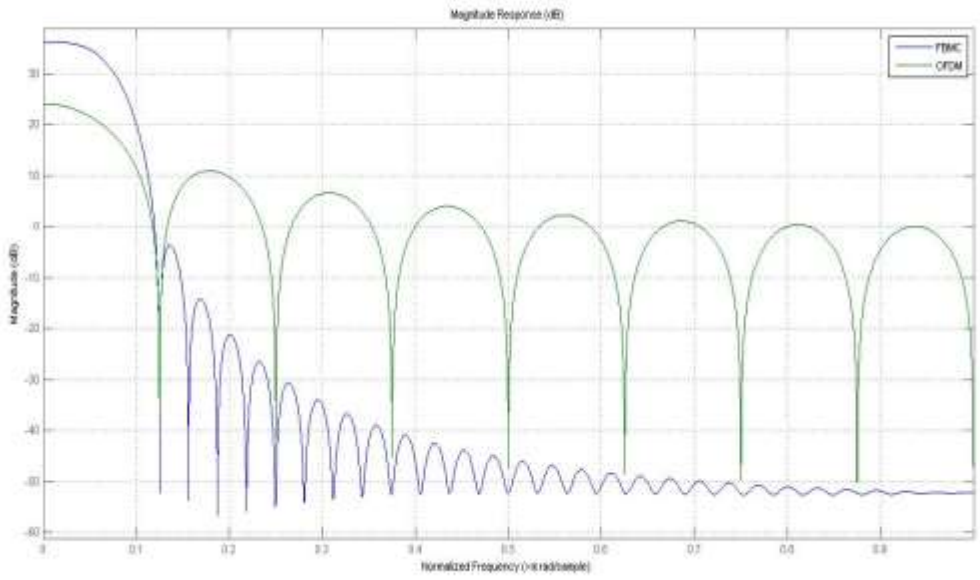

Figure 2.7: Frequency response of prototype filter for FBMC and OFDM

2.4 FBMC-OQAM Polyphase Structure:

The direct form implementations of FBMC are not very efficient for practical applications. The synthesis filter bank (SFB) and the analysis filter bank (AFB) of FBMC/OQAM wireless system introduce high computational complexity because they are performed at the high sampling rate leading to a huge amount of unnecessary calculations. Nevertheless, the computational complexity can be reduced by exploiting polyphase representations of SFB and AFB with IFFT/FFT operations. The polyphase implementation can offer drastic simplifications because filtering operations are done at the lower sampling rate and avoiding unnecessary calculations.

The polyphase filter can be written as follows:

$$\alpha_k[m] = \exp\left(\frac{j2\pi k}{M}\left(m - \frac{L_p - 1}{2}\right)\right)$$

$$= \exp\left(-\frac{j2\pi k}{M}\left(\frac{L_p - 1}{2}\right)\right)\exp\left(\frac{j2\pi km}{M}\right)$$

$$= \beta_k \Upsilon_k[m]$$

Here, we can easily separate the Υ_k and $\beta_k[m]$.

Let assume $m = q + tM$, where $q = 0,1, \dots, M-1$ and $t = 0,1, \dots, K-1$

It can be measured that $\Upsilon_k[m] = \Upsilon_k[q + tM]$, then the k^{th} synthesis filter $G_k(z)$ can be expressed in the form of polyphase filters as follows:

$$G_k(z) = \sum_{m=0}^{L_p-1} p[m]\alpha_k[m]z^{-m}$$

After simplifying the above equation, we get,

$$G_k(z) = \beta_k \sum_{q=0}^{M-1} \Upsilon_k[q]\, z^{-q}\, A_q(z^M)$$

We can denote this form in matrix notation as:

$$G(z) = \boldsymbol{\beta}.\boldsymbol{W}.\boldsymbol{A}(\boldsymbol{z}).\boldsymbol{O}(\boldsymbol{z})$$

Where,

$$G(z) = [G_0(z)G_1(z) \dots \dots G_{M-1}(z))]^T$$

$$\beta = diag[\beta_0\beta_1 \dots \dots \beta_{M-1}]$$

$$W = M\boldsymbol{\Upsilon_k}(\boldsymbol{q})$$

$$A(z) = diag[A_0(z)A_1(z) \dots \dots A_{M-1}(z)]$$

$$O(z) = [1\ z^{-1}\ \dots \dots z^{-(M-1)}\ ]^T$$

Above equation shows that the synthesis filter bank consists of $\beta_k[n]$ multiplies, IFFT, synthesis polyphase filtering $A_q(z)$, up-samplers by $M/2$ and delay chain. It can be noticed that the up-samplers and delay chain form a parallel-to-serial (P/S) converter with overlapping of $M/2$. This is because the

number of branches is M and the up-sampling factor is only $M/2$. So, SFB block with polyphase structure is shown below:

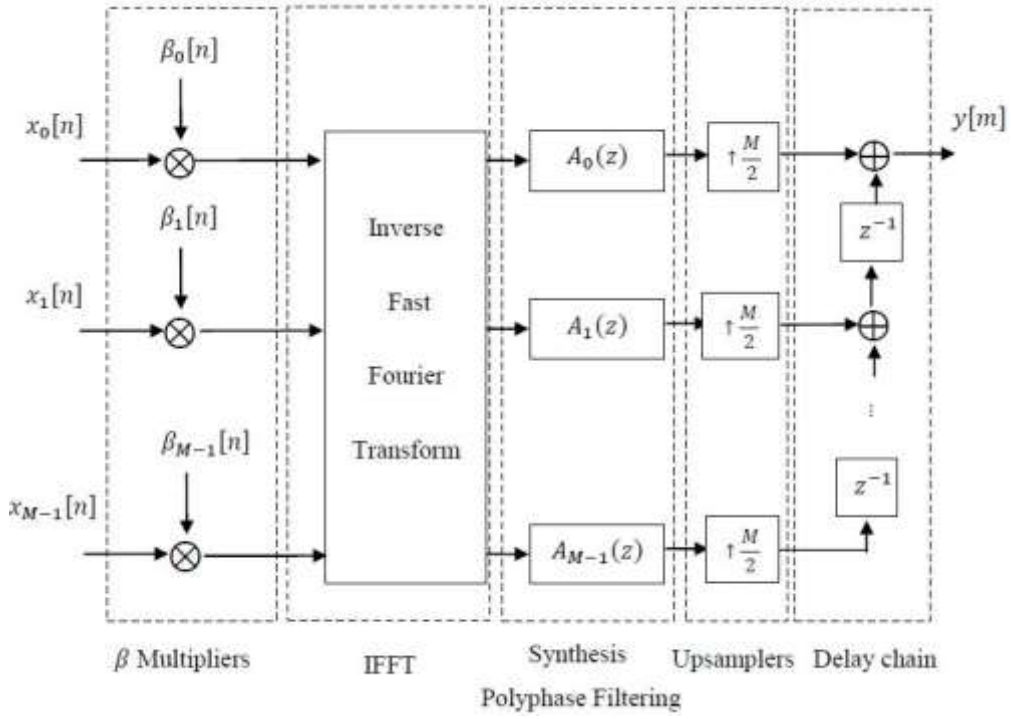

Figure 2.8: SFB using polyphase structure for FBMC-OQAM

Similarly, we can also define the polyphase decomposition of the k^{th} analysis filter $F_k(z)$.

$$F_k(z) = \sum_{m=0}^{L_p-1} p\big[L_p - 1 - m\big]\alpha_k{}^*\,[m]z^{-m}$$

$$F_k(z) = \beta_k{}^* \sum_{q=0}^{M-1} \Upsilon_k{}^*\,[q]z^{-(M-1-q)}B_q(z)$$

Where $B_q(z) = A_{M-1-q}(z)$.

In matrix form, $$F(z) = \beta^*.W^*.B(z).N(z)$$

$$F(z) = [F_0(z)F_1(z) \dots \dots F_{M-1}(z))]^T$$

$$B(z) = diag[B_0(z)B_1(z) \dots \dots B_{M-1}(z)]$$

$$N(z) = [z^{-(M-1)} \;\; z^{-(M-2)} \dots \dots \; z^{-1} \; 1]^T$$

Above equation suggests that the analysis filter bank (AFB) consists of delay chain, down-samplers by $M/2$, analysis polyphase filtering $B_q(z)$, FFT and $\beta_k^*[n]$ multipliers. The analysis polyphase filter at the receiver in time index can be written as follows:

$$b_k(m) = a_{M-1-k}(m) = p(M-1-k+mM)$$

Now, we can define the AFB block with polyphase structure, which is:

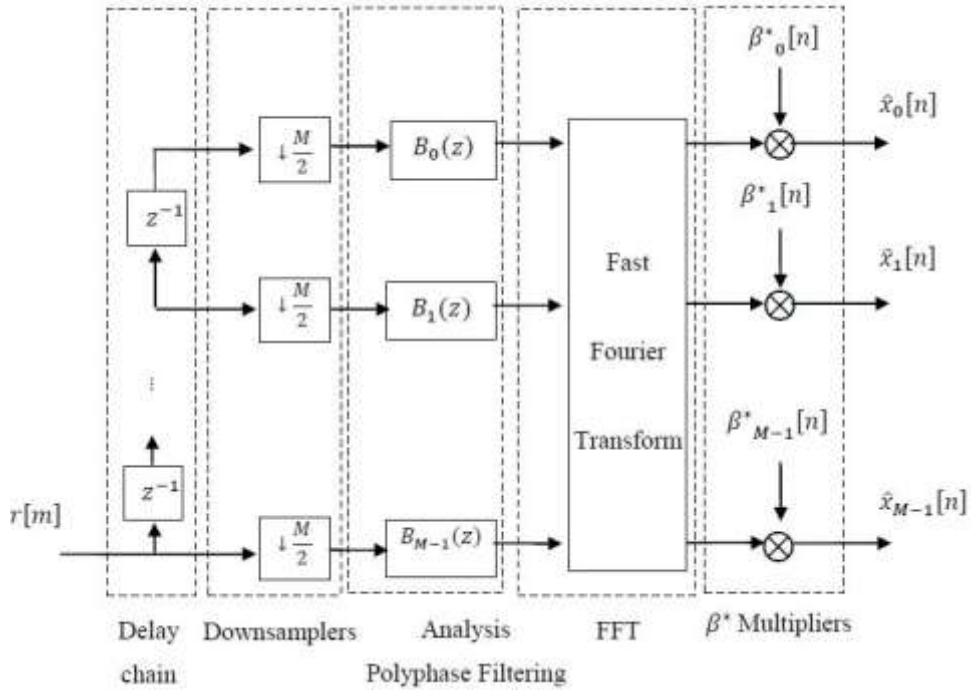

Figure 2.9: AFB using polyphase structure for FBMC-OQAM

2.5 FBMC vs OFDM Subcarriers:

The main difference between FBMC and OFDM is the choice of the prototype filter. The OFDM system uses a rectangular window filter whereas the FBMC system uses a prototype filter designed with the Nyquist pulse shaping principle. This results in negligible ISI and ICI. Because of using well shaped

prototype filter in FBMC, the side-lobe levels are considerably lower than in the case of OFDM. In this way, a good spectral containment for all the sub-channels can be obtained and this also results in a good resistance against narrowband interference. A brief sub-channel comparison between FBMC/OQAM (for overlapping factor $K = 2, 3\ and\ 4$) and OFDM with matlab simulation was observed. Result is shown as follows: X-axis = Normalized frequency (xπ rad/sample), Y-axis= Magnitude (dB) (normalized to 0 dB)

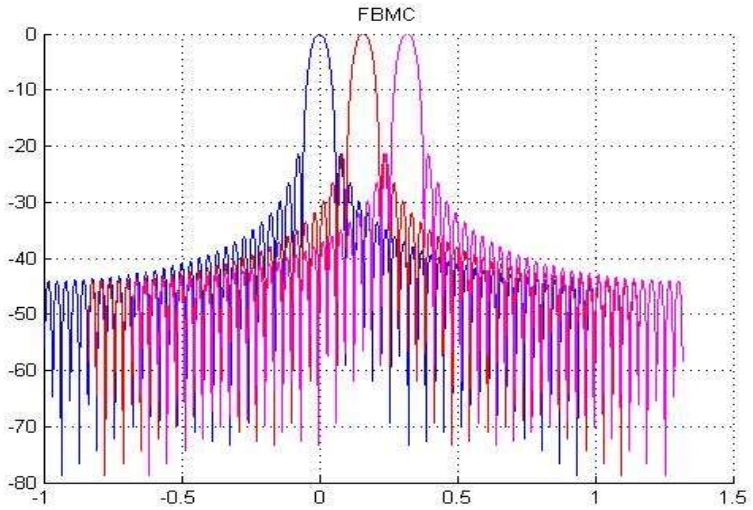

Figure 2.10: FBMC/OQAM Sub-carriers with K=2

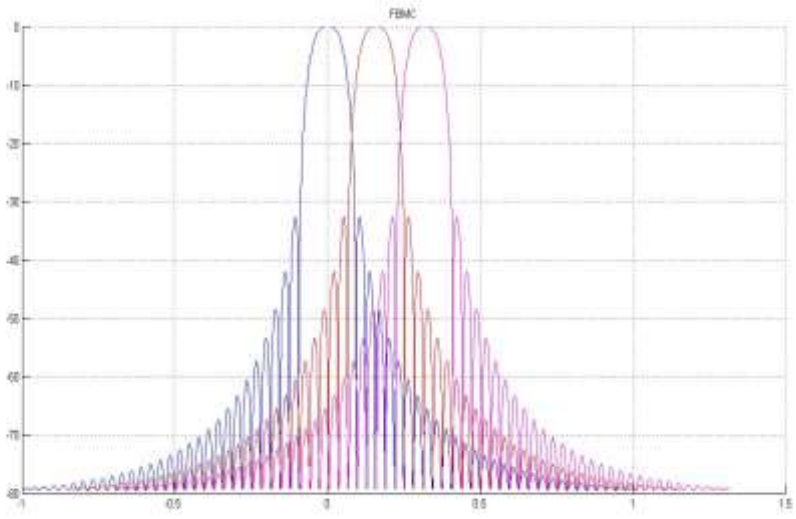

Figure 2.11: FBMC/OQAM Sub-carriers with K=3

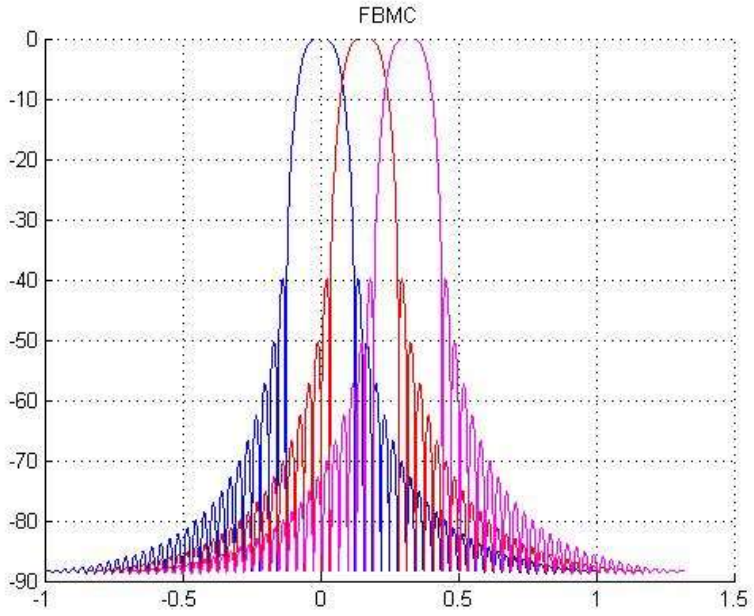

Figure 2.12: FBMC/OQAM Sub-carriers with K=4

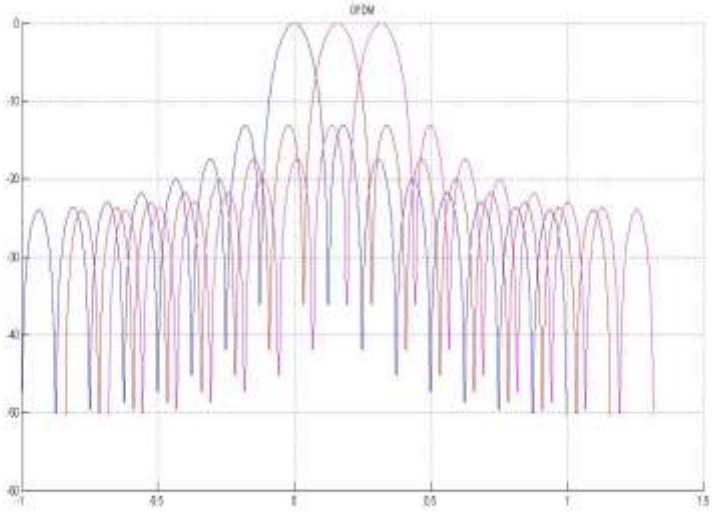

Figure 2.13: OFDM Sub-carriers plot

2.6 Computational Complexity FBMC/OQAM vs. OFDM:

Polyphase is one of technique to reduce computational complexity in FBMC/OQAM system. When polyphase structure is included in FBMC/OQAM system, then the total number of real multiplications for SFB (O_{SFB}) is the sum of the multiplications in each processing block: pre-processing, β_k multipliers, M point IFFT, and M branch polyphase filter section, i.e.

$$O_{SFB} = 2(2M + ((\log_2(M) - 3) + 4) + 2KM)$$

The complexity of AFB is equal to the complexity of SFB because similar processing blocks are used in the reverse order. So, total complexity of the FBMC/OQAM system is given as follows:

$$O_{FBMC/OQAM\ with\ polyphase} = 4(2M + ((\log_2(M) - 3) + 4) + 2KM)$$

Complexity of FBMC/OQAM without polyphase structure is given as follows:

$$O_{FBMC/OQAM\ with\ polyphase} = 4(M.KM)$$

But, the computational complexity of OFDM system is still lower than FBMC/OQAM system with polyphase implementation because it uses IFFT and FFT as modulation and demodulation. So, the complexity of OFDM system can be defined as follows:

$$O_{OFDM} = 2((\log_2(M) - 3) + 4)$$

The Matlab simulation involving complexity of both systems is plotted in following figure.

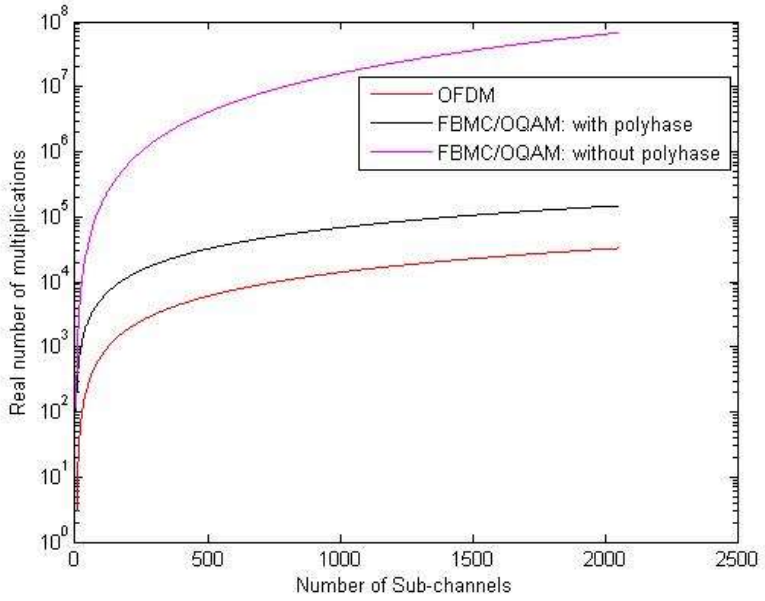

Figure 2.14: Number of real multiplication as a function of number of sub-channels for FBMC and OFDM

2.7 Bit Error Rate (BER) of FBMC-OQAM:

In theoretical, BER performance of FBMC/OQAM is better than OFDM system because FBMC/OQAM system uses a prototype filter designed with the Nyquist pulse shaping principle, which can reduce greatly the spectral leakage problem of OFDM.

Number of subcarriers = 64, SNR=0:5, number of OQAM sample per symbol=2, K=4

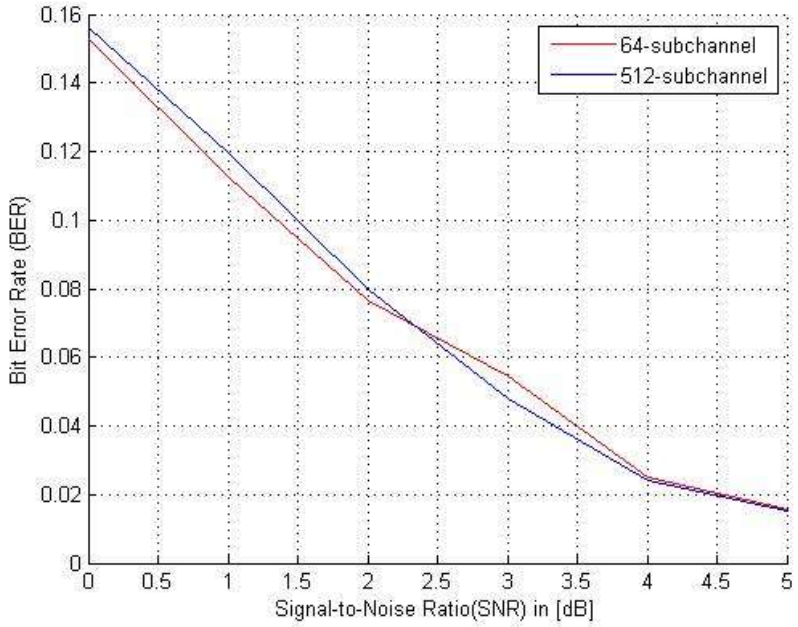

Figure 2.15: BER vs SNR performance of FBMC/OQAM For different sub-carriers

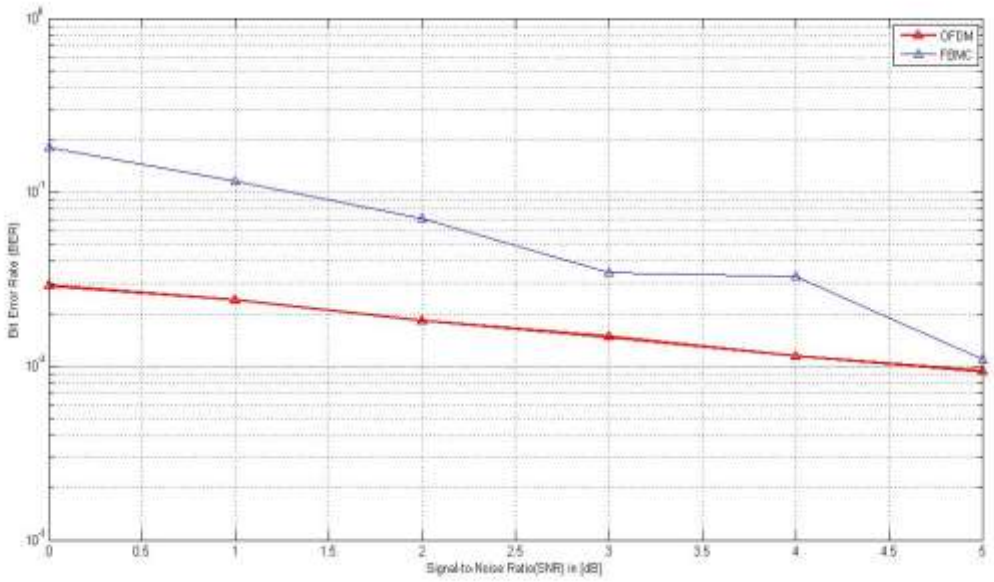

Figure 2.16: BER vs. SNR performance of FBMC/OQAM and OFDM for 64 sub-carriers

CHAPTER 3

PAPR Reduction in FBMC-OQAM systems

In general, the PAPR of a continuous time baseband transmit signal $x(t)$ is defined as the ratio of the maximum instantaneous power to its average power. To better approximate the PAPR of a continuous time transmit signal, the discrete time OFDM signal is to be obtained by L times oversampling. The oversampled discrete time OFDM signal can be obtained by performing LN point IFFT on the data block with $(L-1)N$ zero padding.

3.1 PAPR Reduction Techniques:

Many PAPR reduction techniques are proposed in the literature. In this section, we investigate some such techniques and discuss their advantages and disadvantages in terms of PAPR reduction capability. The PAPR reduction schemes are majorly divided into two categories

a) Distortion Based Techniques
b) Non-distortion Techniques

3.1.1 Distortion Based Techniques:

Distortion based techniques are the most straightforward PAPR reduction methods. These techniques distort the spectrum, this spectrum distortion or "spectral re-growth" can be corrected to a certain extent by using filtering operation. In case of OFDM, clipping and filtering and companding are used to reduce PAPR to the desired level.

3.1.2 Non Distortion Based Techniques:

These types of PAPR reduction schemes do not distort the shape of the OFDM signal and therefore no spectral re-growth take place. There are several methods which can reduce PAPR to the desired level. Like, Partial Transmit Sequence (PTS), Selected Mapping (SLM), Tone Rejection and Tone Injection and many more.

3.2 Classical Selected Mapping (SLM):

In classical SLM scheme for OFDM, the transmitter generates a set of sufficiently different candidate data blocks, all representing the same information as the original data blocks, and selects the most favourable for the transmission. Each symbol is rotated with different phase rotation vectors that are i.i.d and the optimally rotated symbol is chosen among others, based on the least PAPR criterion. The input symbol is phase rotated by U vectors of size LN each (where L is oversampling factor and N is number of subcarriers). These U rotated input symbols carry same information and pose identical constellation like the original input symbols. After the modulation, the PAPR is calculated over an OFDM symbol period and the symbol with the least PAPR is chosen, which is referred as optimally rotated symbol.

3.2.1 Example:

Here, we show a simple example of the SLM technique for an OFDM system with eight subcarriers. We set the number of phase sequences to U = 4. The data block to be transmitted is denoted $\mathbf{X} = [1, -1, 1, 1, 1, -1, 1, -1]'$ whose PAPR before applying SLM is 6.5dB. We set the four phase factors as $\mathbf{B}(1) = [1, 1, 1, 1, 1,$
$1, 1, 1]'$. $\mathbf{B}(2) = [-1, -1, 1, 1, 1, 1, 1, -1]'$. $\mathbf{B}(3) = [-1, 1, -1, 1, -1, 1, 1, 1]'$, and $\mathbf{B}(4) = [1, 1, -1, 1, 1, -1, 1, 1]'$. Among the four modified data blocks $\mathbf{X}(u)$, u = 1, 2, 3, 4, $\mathbf{X}(2)$, has the lowest PAPR of 3.0dB. Hence, $\mathbf{X}(2)$ is selected and transmitted to the receiver. For this data block, the PAPR is reduced from 6.5 to 3.0 dB, resulting in a 3.5 dB reduction. In this case, the number of IDFT

operations is 4 and the amount of side information is 2 bits. The amount of PAPR reduction may vary from data block to data block, but PAPR reduction is possible for all data blocks.

3.3 Dispersive Selected Mapping (SLM):

In dispersive SLM, each symbol is rotated with different phase rotation vectors that are i.i.d similar to the classical SLM scheme. After that, the optimally rotated symbol is chosen among others based on least PAPR that has been calculated over $[0, 4T)$ instead of $[0, T)$. This method can be used for any prototype filter such as IOTA (Isotropic Orthogonal Transform Algorithm). The algorithm of DSLM method is explained in following steps,

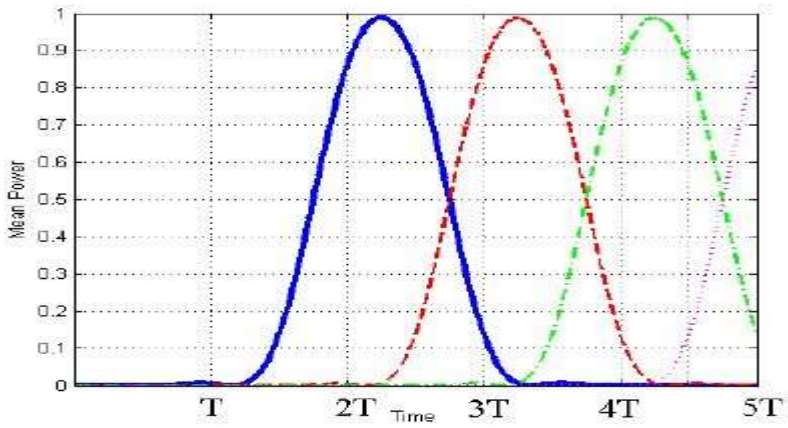

Figure 3.1: mean power overlapping among FBMC-OQAM symbols

Step 1 (Initialization):

At first, we generate U phase rotation vectors of length N as, $B^{(u)} = [b_{u,0}, b_{u,1}, \dots\dots, b_{u,N-1}]^T$ and $u = 1, 2, \dots\dots, U$

Where, without loss of generality, we choose $B^{(1)} = 1$.

Step 2 (Rotation):

We can get modified data symbols for the uth sequence by point-to-point multiplication of each input symbol with phase rotation vector.

$$X^{(u)} = \mathrm{X} * B^{(u)}$$

$X = [X_0, X_1, \dots\dots, X_{N-1}]$ is input symbol.

Step 3 (Modulation):

We modulate the mth input symbol of FBMC-OQAM considering the overlap of previous symbol.

$$x^{(u)}(\boldsymbol{t}) = \sum_{n=0}^{N-1} \sum_{m'=0}^{2m-1} (overlapping\ past\ symbols) s_k[n]\, p_T(t - nT) \exp(j2\pi(t - nT) f_k) * B^{(u)} + \sum_{n=0}^{N-1} \sum_{m'=2m}^{2m+1} (Current\ symbol) s_k[n]\, p_T(t - nT) \exp(j2\pi(t - nT) f_k) * B^{(u)}$$

Step 4 (PAPR Calculation):

In this part, we calculate the PAPR of transmitted signal over an interval of T_0,

Where T_0 is an arbitrary interval that includes $[mT, mT + 4T]$ interval because of overlapping structure of FBMC-OQAM symbols.

Information about the selected phase sequence should be transmitted to the receiver as side information. At the receiver, the reverse operation is performed to recover the original data block.

$$U_{SI} = U_{SI} * u_{min}$$

The vector U_{SI}, which is a null vector initially. And it will be updated for every m^{th} symbol by row concatenation with previously obtained u_{min}.

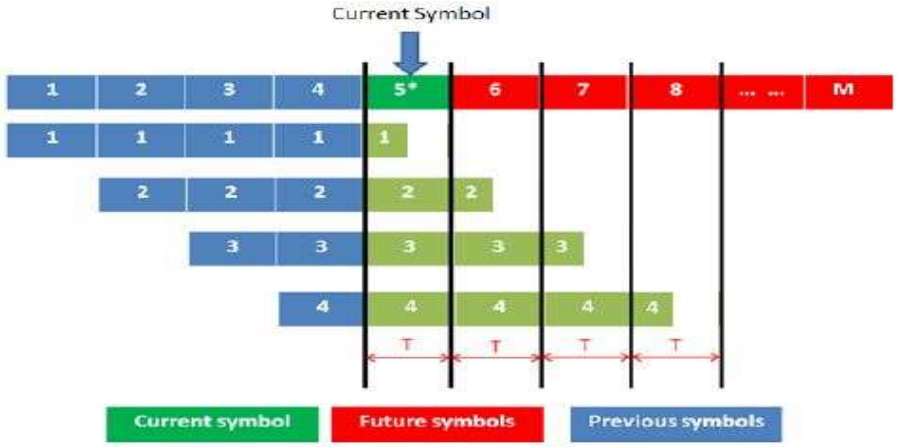

Figure 3.2: Block diagram of Dispersive SLM for FBMC-OQAM systems

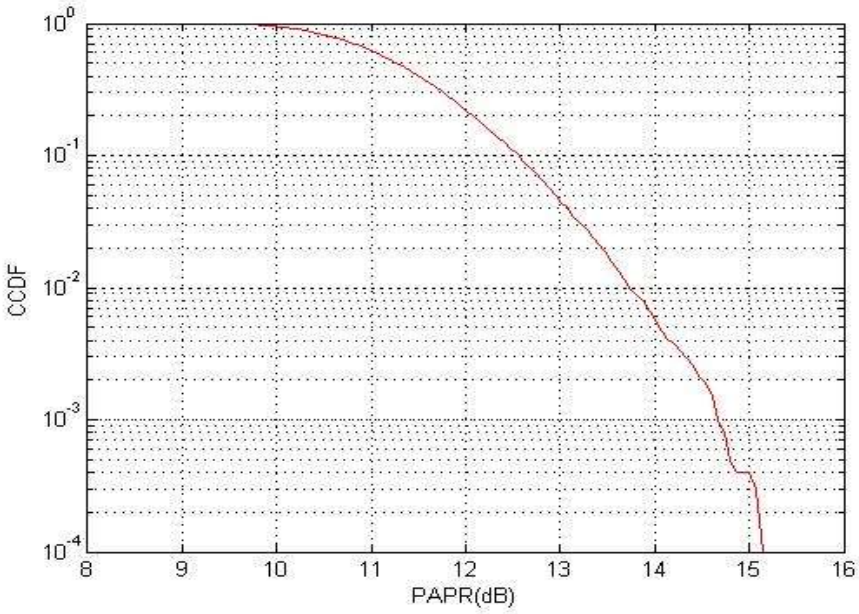

Figure 3.3: CCDF of PAPR for FBMC/OQAM system

CHAPTER 4

Channel Estimation and Equalization

4.1 Channel Model:

Wireless communication channels affect the input signals in different way, such as linear and nonlinear distortion, additive random noise, fading and interference. The channel can be modeled as a linear time invariant (LTI) system followed by a zero mean additive white Gaussian noise (AWGN) source.

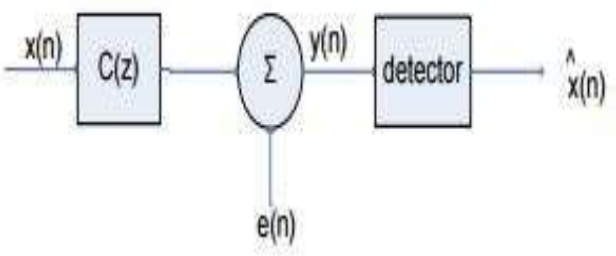

Figure 4.1: Channel model block diagram

$x(n)$ is assumed to be consisted of the sum of M sequences, each transmitted in one of M sub-channels. We can write this,

$$\mathrm{x(n)} = \sum_{k=0}^{M-1} \mathrm{x_k}(n)$$

The output of the channel can be calculated as follows:

$$y(n) = x(n) * c(n) + e(n)$$

The received signal $y(n)$ is a noisy and distorted signal version of the input signal $x(n)$. $\hat{x}(n)$ is the estimated value which is the output of the detector, but may it will be not identical to the transmitted signal because of ISI caused by

channel which is because of multipath fading and limitation in bandwidth, and noise $e(n)$, this will give us a nonzero probability of error P_e. The channel model parameters are given in Table 2.1.

	Ped B		Veh A	
p	path power $P_{l,p}$ [dB]	path delay $\tau_{l,p}$ [ns]	path power $P_{l,p}$ [dB]	path delay $\tau_{l,p}$ [ns]
0	0	0	0	0
1	-0.9	200	-1	310
2	-4.9	800	-9	710
3	-8	1200	-10	1090
4	-7.8	2300	-15	1730
5	-23.9	3700	-20	2510

	Veh A extended		Veh B	
p	path power $P_{l,p}$ [dB]	path delay $\tau_{l,p}$ [ns]	path power $P_{l,p}$ [dB]	path delay $\tau_{l,p}$ [ns]
0	0	0	-2.5	0
1	-1	310	0	300
2	-9	710	-12.8	8900
3	-10	1090	-10	12900
4	-15	1730	-25.2	17100
5	-20	10000	-16	20000

Table 4.1: Power Delay Table of channel model

I have used a random uniform channel generated in MATLAB.

```
h = randn(numTaps,1);
```

Also, Rayleigh channel is used to tackle the problem of fading. Beside the choice of the model the speed of the user is an important measure for characterising the channel. Frequency selectivity is dominantly influenced by the choice of the model, time variance by the speed. Another important feature of modelling wireless channels is the correlation between the different antenna links.

```
%Rayleigh channel
Ts=1e-4; % sampling time in second
Fd=100; % doppler frequency in Hz
h = rayleighchan(Ts, Fd, Tau, PdB);
```

4.2 Channel Equalization Techniques:

We will use a least mean square (LMS) algorithm which is based on cost functions, mean-squared error (MSE) adapted for FBMC system with offset QAM modulation (OQAM). In this method, we can achieve an adaptive equalizer with minimum complexity because of applying the equalizer to each sub-carrier.

4.2.1 Least Mean Squares (LMS):

The LMS algorithm is used as adaptive equalizer based on mean square error (MSE) for each sub-channel. Also, a per-subcarrier equalizer works at $T/2$, where T is the symbol duration. The best part is that the only parameter to be adjusted is the adaptation step size α. Through an iterative process, all filter tap weights are adjusted during each sample period in the training sequence. At last, the filter will reach a value that minimizes the mean square error (MSE) between the equalized signal and the stored input signal. We will see from the result that the choice of α involves a trade-off between rapid convergence and MSE. A large α value can result in a system that converges rapidly on start-up, but then chops around the optimal coefficient at steady state. To tackle the problem of ISI and ICI, we will use one FIR equalizer per subcarrier. The LMS equalizer is used to minimize the MSE between the desired output of the equalizer and the actual output equalizer.

We will apply the equalizer to the real and imaginary parts for each subcarrier separately. The filter weights are updated as in the below equation. The least mean squares can be computed iteratively by,

$$s_k(n) = w'_N(n) y_N(n)$$

$$e_k(n) = x_k(n) - s_k(n)$$

$$w_N(n+1) = w_N(n) - \alpha * e_k{}^*(n) * y_N(n)$$

Now, we can calculate the mean square error (MSE) at instance time k

$$MSE = E[e_k{}^* e_k]$$

4.3 Channel Estimation Techniques:

Adaptive estimation of channel is necessary before the demodulation of multi-carrier FBMC/OQAM signals since the wireless channel is frequency selective and time varying. There are two main problems in designing estimators for wireless any multi-carrier systems. The first problem is the arrangement of pilot information, where pilot means the reference signal used by both transmitter and receiver. The second problem is the design of an estimator with both low complexity and good channel tracking ability. The combination of high data rates and low bit error rates in FBMC/OQAM systems constrains the use of estimators that have both low complexity and high accuracy, and we find a good trade-off between these two constraints. In FBMC/OQAM systems to get a good trade-off between complexity and accuracy we use one-dimensional channel estimators. It can be categorized in two forms

- Pilot based channel estimation
- Blind channel estimation methods

Pilot based channel estimation has two categories block-type pilot channel estimation and comb-type channel estimation, in which the pilots are inserted in the frequency direction and time direction, respectively. Least Squares (LS), minimum mean-square error (MMSE) can be used to estimate for the block-type pilot arrangement. Pilot based channel estimation methods are easy to implement compare to blind channel estimation methods, but they reduce bandwidth efficiency.

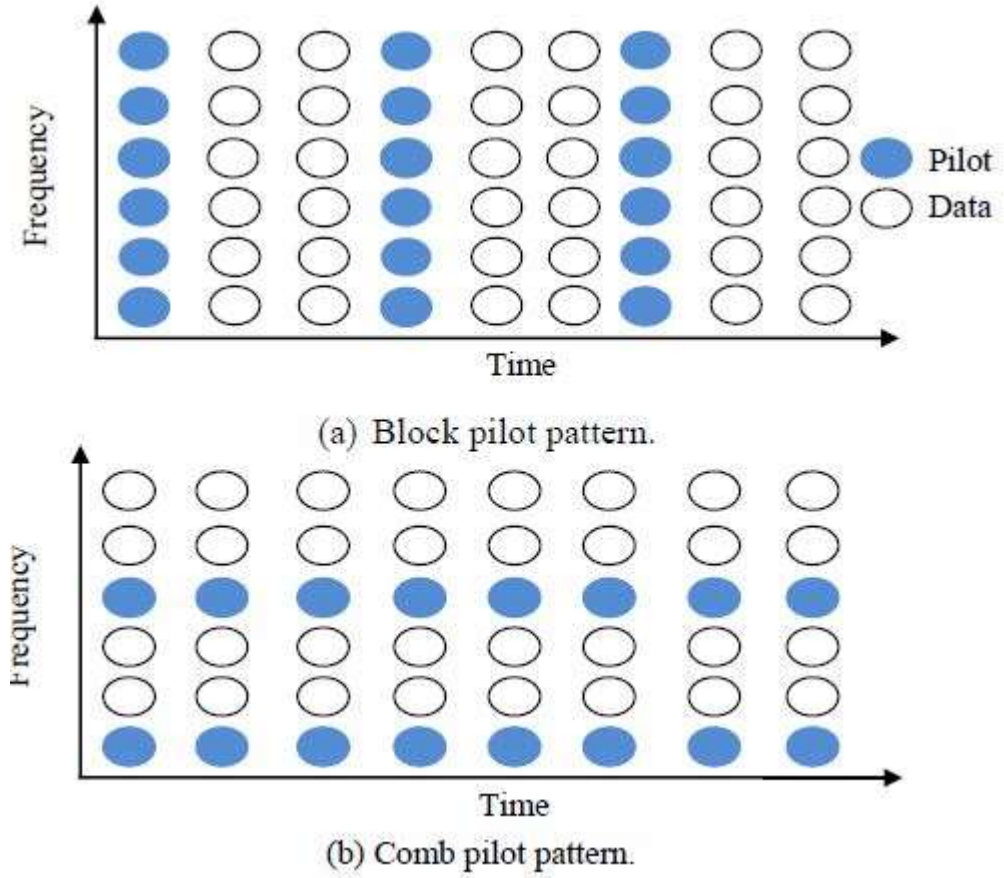

Figure 4.2: Pilot patterns structure

4.3.1 General Form of MMSE and LS Estimators:

4.3.1.1 Minimum mean square error (MMSE) estimator:

Let's assume that the channel is time-invariant, but frequency selective. Also, in the pilot based methods it is assumed that the preamble is known at the

receiver. The channel estimation is done in the preamble symbol. The received symbol at pilot carriers is given by

$$y[k] = x[k]H[k] + w[k]$$

Where $x[k]$, $y[k]$, $H[k]$, $w[k]$ are the transmitted symbol, the received symbol, the channel transfer function and complex zero mean white Gaussian noise at the k^{th} sub-carrier. The above equation can be written as follows,

$$y = XFh + w$$

Let N_p be the number of pilots. X is a diagonal matrix containing the elements $x[k]$, F is the DFT matrix and h is the channel impulse response.

Here, it can be assumed that channel vector h is Gaussian and uncorrelated with the channel noise w, so the MMSE estimate of h will be

$$\hat{\mathrm{h}}_{MMSE} = R_{hy}{R_{yy}}^{-1}y$$

R_{hy} and R_{yy} are the cross-covariance matrix between h and y and the auto-covariance matrix of y respectively.

$$R_{hy} = \mathrm{E}\{\mathrm{h}y^H\} = R_{hh}F^H X^H$$

$$R_{yy} = \mathrm{E}\{\mathrm{y}y^H\} = XFR_{hh}F^H X^H + {\sigma_n}^2 I_N$$

Further, R_{hh} is the auto-covariance matrix of h and ${\sigma_n}^2$ represents the noise variance $E\{|n_k|^2\}$.

Since the columns in F are orthogonal, $\hat{\mathrm{h}}_{MMSE}$ generates the frequency-domain MMSE estimate H_{MMSE} by

$$H_{MMSE} = \mathrm{F}\hat{\mathrm{h}}_{MMSE} = FQ_{MMSE}F^H X^H y$$

Where Q_{MMSE} is given as follows

$$Q_{MMSE} = R_{hh}[(F^H X^H XF)^{-1}{\sigma_n}^2 + R_{hh})]^{-1}(F^H X^H XF)^{-1}$$

If g is not Gaussian, H_{MMSE} is not necessarily a minimum mean-square error estimator. It is however the best linear estimator in the mean-square error sense.

4.3.1.2 Least Square (LS) Estimator:

Similarly, the LS estimator for the cyclic impulse response h minimizes $(\mathrm{y} - \mathrm{XFh})^{\mathrm{H}}(\mathrm{y} - \mathrm{XFh})$ and generates

$$\mathrm{H_{LS}} = \mathrm{FQ_{LS}F^{H}X^{H}y}$$

Where

$$\mathrm{Q_{LS}} = (\mathrm{F^{H}X^{H}XF})^{-1}$$

$$\mathrm{H_{LS}} = \mathrm{X^{-1}y}$$

We can also compute LS estimate of its error covariance matrix.

CHAPTER 5

Simulation Results

5.1 Overview

In this chapter, we present a comparative simulation on PAPR reduction in FBMC-OQAM using dispersive selected mapping (DSLM). It utilizes the overlapping property of FBMC-OQAM signals and the time dispersive nature of the FBMC-OQAM symbols.

We will use a least mean square (LMS) algorithm which is based on cost functions, mean-squared error (MSE) adapted for FBMC system with offset QAM modulation (OQAM). In this method, we can achieve an adaptive equalizer with minimum complexity because of applying the equalizer to each sub-carrier. We observed that the MSE in this channel model with step size 0.007 converges rapidly which is better than with 0.01 which converges slower than before. We also observed that same subcarrier could have good characteristics curve at some step sizes of the equalizer and bad characteristics at another step sizes.

We also perform channel estimation of FBMC-OQAM systems based on least squares (LS) and minimum mean square errors (MMSE) channel estimators. The FBMC-OQAM with poly-phase structure has been carried out and simulated using MATLAB with different parameters.

In this part, we carry out a comparative simulation study on the channel estimation of FBMC/OQAM based on the conventional Least Squares (LS) and linear minimum mean square error (LMMSE) channel estimators. The mean square error (MSE) result versus signal-to-noise ratio (SNR) for estimation

techniques LS and LMMSE is shown below in figures. Also, the bit error rate (BER) result versus signal-to-noise ratio (SNR) for estimation techniques LS is shown below in figure.

5.2 PAPR reduction performance

FBMC-OQAM uses dispersive SLM instead of classical SLM to reduce the PAPR. Similar to the classical SLM scheme, each symbol is rotated with different phase rotation vectors that are i.i.d and the optimally rotated symbol is chosen among others based on least PAPR criterion that has been computed over $[0,4T)$ instead of $[0,T)$. Complementary cumulative distributive function (CCDF) of PAPR plot for FBMC-OQAM signals with PAPR calculated over $[0,4T)$ with rotation vector, U=4. We can object from this figure that, when dispersive SLM technique is used to reduce PAPR, then it leads to an improvement.

Fig. 5.1 shows the CCDF of PAPR plot based on Dispersive SLM

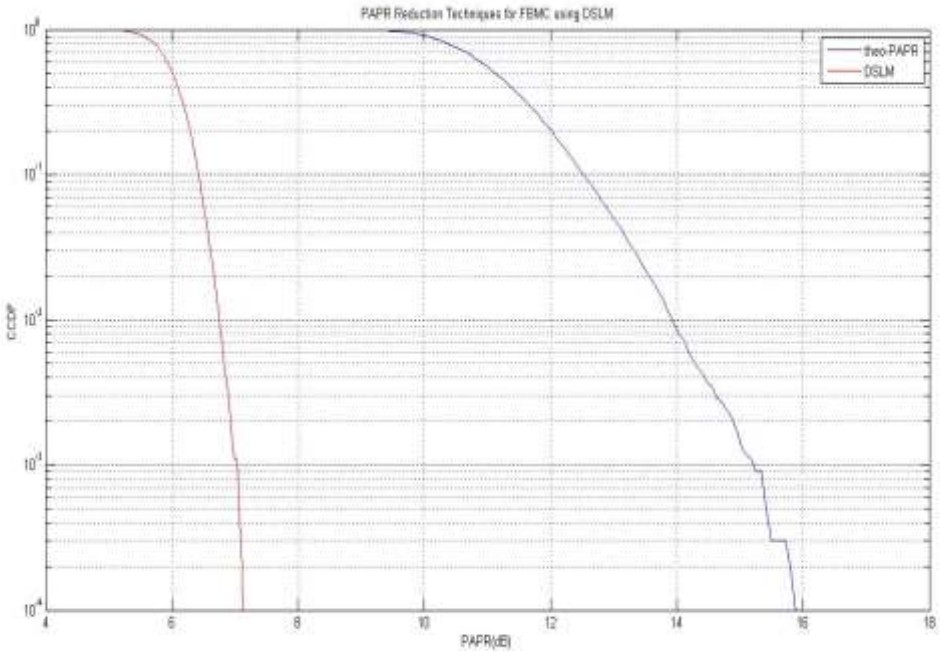

Figure 5.1: CCDF of PAPR plot for FBMC-OQAM

5.3 Channel Equalization Results

Fig. 5.2 shows the FBMC-OQAM transmitted symbols and received symbols after channel but before equalization.

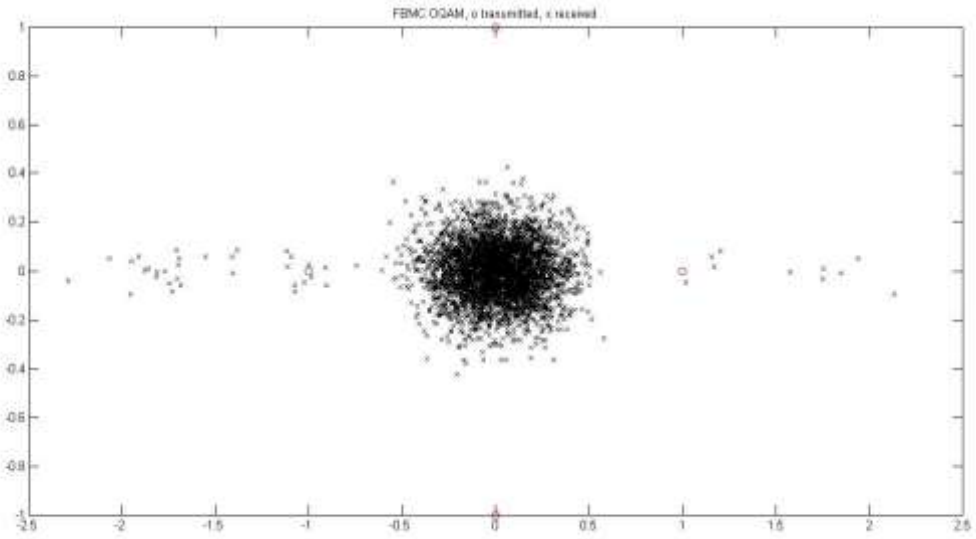

Figure 5.2: Transmitted and Received Symbols plot for FBMC-OQAM

Fig. 5.3 shows the output estimation error plot vs. number of iteration based on least mean square (LMS) adaptation learning algorithm for FBMC-OQAM.

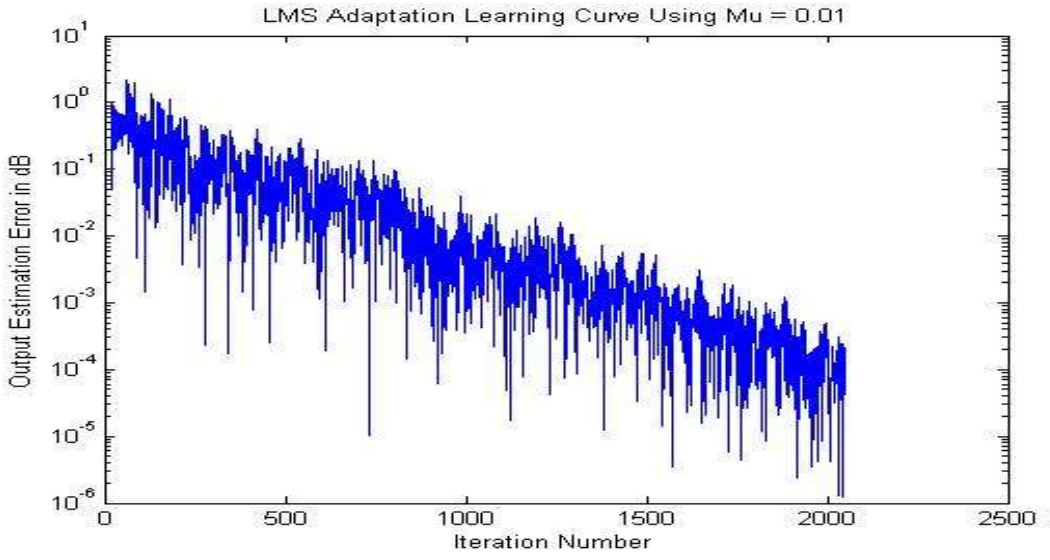

Figure 5.3: Output Estimation Error plot for FBMC-OQAM based on LMS

Fig. 5.4 shows the mean square error (MSE) plot vs. number of iteration based on least mean square (LMS) adaptation learning algorithm for FBMC-OQAM

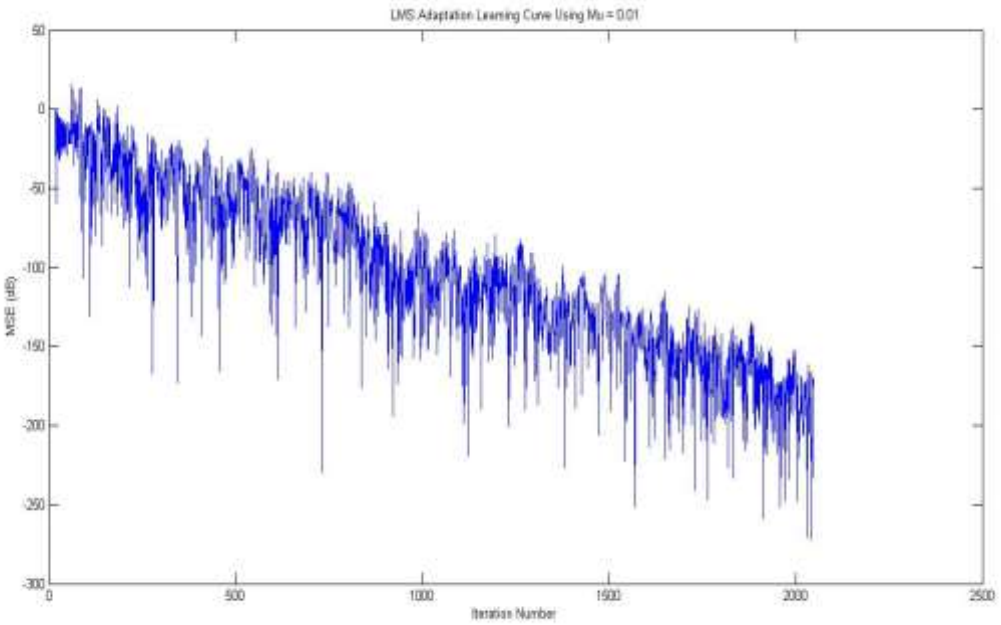

Figure 5.4: MSE plot for FBMC-OQAM based on LMS

Fig. 5.4 shows the bit error rate (BER) plot vs. signal to noise ratio (SNR) before equalization based on least mean square (LMS) adaptation learning algorithm for FBMC-OQAM.

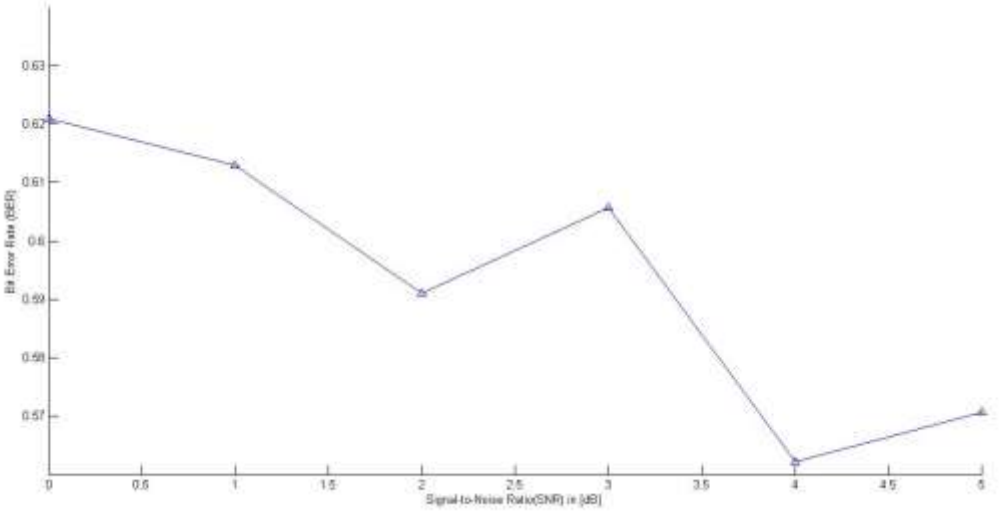

Figure 5.5: BER vs. SNR plot for FBMC-OQAM before equalization

Fig. 5.4 shows the bit error rate (BER) plot vs. signal to noise ratio (SNR) after equalization based on least mean square (LMS) adaptation learning algorithm for FBMC-OQAM.

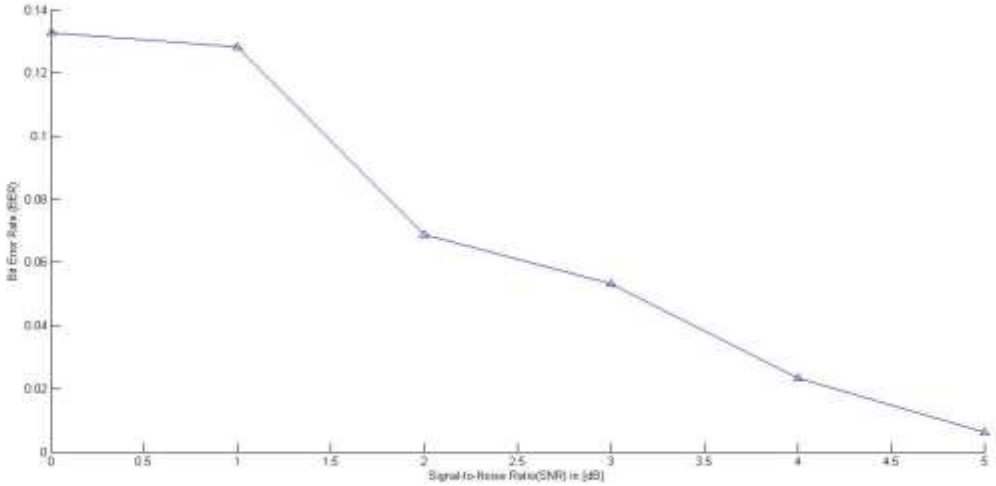

Figure 5.6: BER vs. SNR plot for FBMC-OQAM after equalization

5.4 Channel Estimation Results

Fig. 5.6 shows the mean square error (MSE) performance vs. SNR plot of FBMC-OQAM system for different estimators

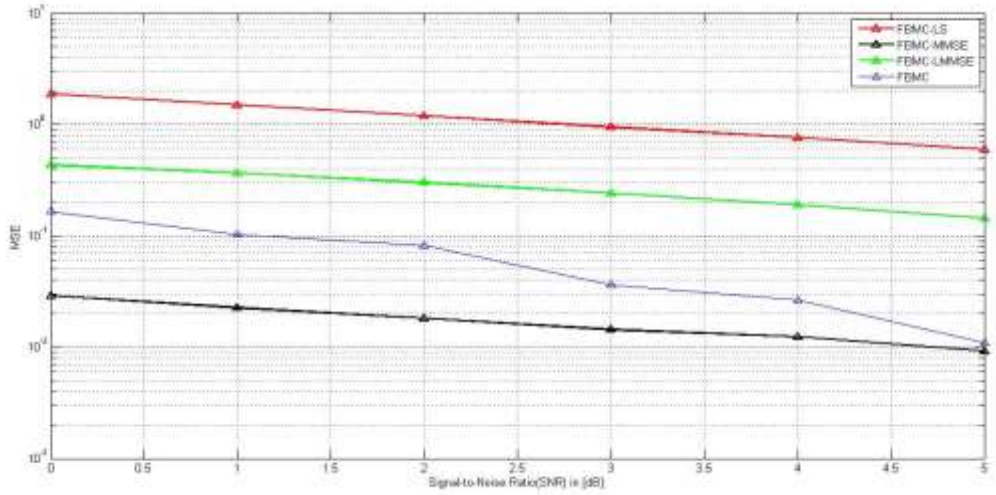

Figure 5.7: MSE vs. SNR plot for FBMC-OQAM for different estimators like LS and MMSE

Fig. 5.7 shows the BER performance vs. signal to noise ratio (SNR) for FBMC-OQAM system based on least square (LS) estimator.

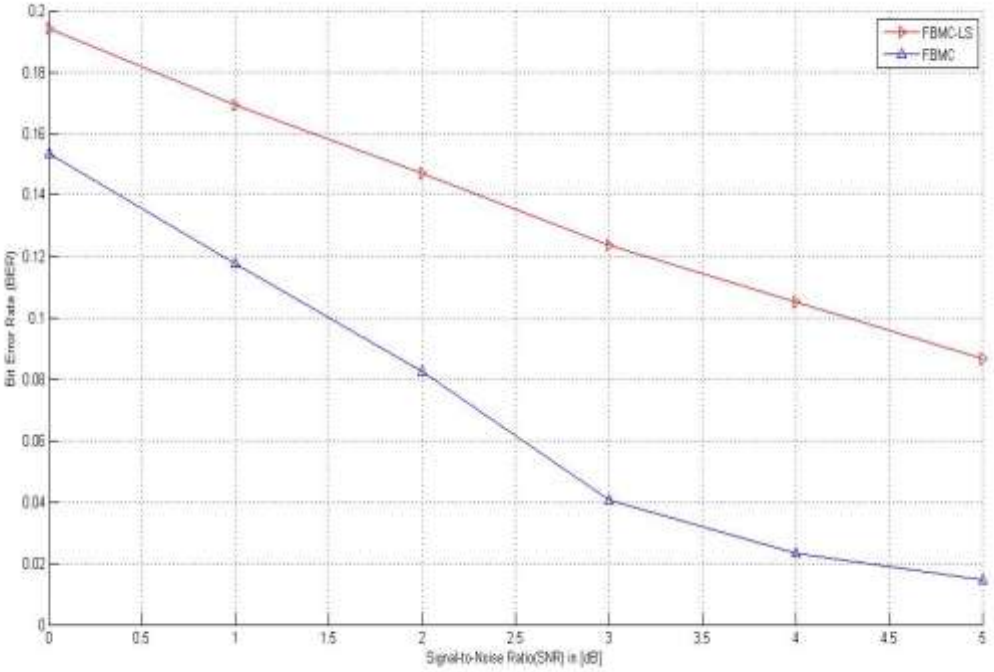

Figure 5.8: BER performance vs. SNR plot for FBMC-OQAM for LS estimators

CHAPTER 6

Conclusion and Future Work

FMBC systems outperform OFDM in terms of spectral efficiency, robustness and bandwidth efficiency at a cost of increased complexity. For example, in the uplink of an OFDM system, carrier and time recovery of signals from different nodes is very necessary and it is a very hard task to achieve. In case of FBMC systems, the perfect carrier and time synchronization between the users can be achieved because it uses signal separation through filtering. FBMC is an elegant method that achieves most of these problems by taking a filtering approach to multicarrier communications. These qualities of FBMC make it an ideal choice for cognitive radio communications, multiple access networks, DSL and PLC. Also, FMT (Filtered Multi-tone) is the only FBMC system that can be efficiently extended for transmission over MIMO channels so far because it uses filter banks with non-overlapping subcarriers.

In this thesis, we use the dispersive SLM to overcome the problem of high PAPR of FBMC-OQAM system. We also use the pilot based channel estimation process. Future research, in this context, will be directed towards the more realistic scenarios of frequency-selective sub-channels and lack of synchronism among nodes in the network. Also, the different kind of training symbols can be modified to estimate the fading channel process.

REFERENCES

1. P. P. Vaidyanathan, Multirate Systems and Filter Banks, Prentice-Hall, Englewood Cliffs, NJ, USA, 1993.

2. FP7-ICT project PHYDYAS- Physical Layer for Dynamic Spectrum Access and Cognitive Radio, http://www.ict-phydyas.org.

3. Bellanger, M., et al. "FBMC physical layer: a primer." PHYDYAS, January (2010).

4. Farhang-Boroujeny, Behrouz. "OFDM versus filter bank multicarrier." Signal Processing Magazine, IEEE 28.3 (2011): 92-112.

5. Aissa Ikhlef and Jerome Louveaux, "An enhanced MMSE per SubChannel Equalizer for highly frequency selective channels for FBMC/OQAM systems", IEEE-2009

6. Equalization and demodulation in the receiver (single antenna)-,"Prototype filter and structure optimization", Phydyas Deliverable 3.1

7. Christos Mavrokefalidis and Eleftherios Kofidis "Preamble-based channel estimation in single-relay networks using FBMC/OQAM" Springer Open Journal 2014.

8. S. S. Krishna Chaitanya BULUSU and Hmaied SHAIEK "Reduction of PAPR for FBMC-OQAM Systems using Dispersive SLM Technique" 2014.

9. Mahmoud Aldababseh "Estimation of FBMC/OQAM Fading Channels Using Dual Kalman Filters" Hindawi 2014